THE ASTROPHYSICAL JOURNAL, 254:221–231, 1982 March 1

THE HOT SUBDWARFS REVISITED

F. WESEMAEL,[1,2] D. E. WINGET,[1] W. CABOT,[1]
H. M. VAN HORN,[1] AND G. FONTAINE[3]

Received 1981 February 2; accepted 1981 September 9

ABSTRACT

The properties and evolutionary status of the hot B and O subdwarfs are reinvestigated using recent homogeneous grids of hot, high-gravity model atmospheres and detailed convective envelope calculations appropriate to the hot subdwarf region of the H-R diagram discussed by Greenstein and Sargent. An alternative method of analysis of the hot subdwarfs is outlined, where comparisons between observations and theoretical evolutionary tracks are made as close to the fundamental observational results as possible, and are performed directly in the observer's (i.e., $[U - B]$ versus $[B - V]$, or $[B - V]$ versus $D[0.1]$ of Hγ) diagram. As an illustrative example of this procedure, we use a set of gravitationally contracting pre–white dwarf evolutionary sequences at $M_*/M_\odot = 0.4$, 0.6, and 0.8 which are found to evolve through the hot subdwarf domain along the extended horizontal branch.

The properties of stars evolving along the extended horizontal branch are discussed. The consequences of interpreting the sdB/sdO transition as a result of convective mixing along that branch are analyzed. The importance of diffusion, which affects both surface abundances and the onset of convective mixing, is emphasized. An upper limit on the evolutionary time scale of sdB stars of $\tau_{\rm sdB} \lesssim 10^5$ years is set on the basis of diffusion arguments. The possibility that hot subdwarfs are progenitors of helium-rich white dwarfs is also considered. Some speculations concerning the evolutionary phases preceding the hot subdwarfs are offered.

Subject headings: stars: atmospheres — stars: early-type — stars: evolution — stars: subdwarfs

I. INTRODUCTION

The hot subdwarfs are stars with characteristics intermediate between the main sequence and the white dwarfs. The hottest of these stars, the sdO's, have helium-dominated atmospheres, while the cooler stars, the sdB's, have hydrogen-dominated atmospheres exhibiting a variety of He/H ratios. This information, along with the continuity of the mass-to-light ratio on the so-called extended horizontal branch (EHB),[4] represents the main constraints which must be satisfied by any attempt at a theoretical interpretation of the hot subdwarfs.

There have been many efforts to find evolutionary tracks in the theoretical H-R diagram which pass through the region appropriate to the hot subdwarfs (cf. Cox and Salpeter 1961; Faulkner 1972; Caloi 1972, 1976; Sweigart, Mengel, and Demarque 1974; Mengel, Norris, and Gross 1975; Hunger *et al.* 1981). Most of the work done prior to 1974 has been nicely summarized by Greenstein and Sargent (1974, hereafter referred to as GS). However, no clear theoretical picture of the evolutionary status of the hot subdwarfs has yet emerged. A major obstacle to the advance of the theoretical work has been the lack of adequate model atmospheres for hot, high-gravity stars. Recently, detailed grids of such models have become available for both H-rich (Wesemael *et al.* 1980) and He-rich (Wesemael 1981) compositions.[5] Along with a few additional models calculated specifically for this paper, these grids provide a preliminary interpretation of the global properties of the hot subdwarfs in terms of monoelemental atmospheres. The procedure followed in this paper involves the transformation directly into the observer's plane (for example, $[U-B]$ versus $[B-V]$) of theoretical evolutionary tracks which evolve along the EHB through the hot subdwarf domain. This procedure permits us to avoid some of the uncertainties inherent to the inverse, and more conventional, transformation from the observational plane to the theoretical H-R diagram.

[1] Department of Physics and Astronomy and C. E. Kenneth Mees Observatory, University of Rochester.

[2] Department of Astronomy, University of Illinois at Urbana-Champaign, and Institute of Astronomy, University of Cambridge.

[3] Département de Physique, Université de Montréal, and Observatoire du Mont Mégantic.

[4] The term "extended horizontal branch" was coined by Greenstein and Sargent (1974) to identify those faint, blue stars which *appear* to be on a blue extension of the horizontal branch observed in globular clusters. According to these authors, the EHB consists of, in order of increasing effective temperature, blue horizontal-branch stars, B subdwarfs, and O subdwarfs. We adopt this terminology here and use the term EHB to describe globally the sdB and sdO stars. This, however, does not imply that the EHB stars are directly related to Population II horizontal-branch stars!

[5] A smaller grid of high-gravity, mixed-composition (He/H = 0.1 and 1.0) models has also been computed by Kudritzki (1976). These models, both LTE and NLTE, were subsequently used by Kudritzki and Simon (1978) and Hunger *et al.* (1981) to carry out detailed analyses of spectra of individual sdO stars.

Another stumbling block in our understanding of hot subdwarfs has been the relative failure of theoretical models with shell-burning sources to account for the EHB in a coherent way (e.g., Sweigart, Mengel, and Demarque 1974). This suggests the possibility that the hot subdwarfs may not be shell-burning objects and that, perhaps, a reexamination of their evolutionary status may be in order. In particular, we believe that the lack of a clear picture of the evolutionary status of stars on the EHB renders evolutionary sequences for evolved, low-mass ($M_* \leq M_\odot$) stars which pass through the hot subdwarf region of considerable interest. In this paper we discuss a set of gravitationally contracting pre–white dwarf evolutionary sequences at $M_* = 0.4$, 0.6, and 0.8 $M_\odot$ which have the virtues that (i) they evolve along the EHB through the hot subdwarf region, and (ii) their details are available to us. While the initial models of these sequences do not readily connect with known previous phases of post–zero-age horizontal branch (ZAHB) evolution and are, in that sense, ad hoc, these sequences are nevertheless of considerable importance in improving our understanding of the physical processes occurring along the EHB, and in illustrating the utility of model atmosphere and envelope calculations for the investigation of the nature of hot subdwarfs. We emphasize, furthermore, that many of the qualitative results presented in the following sections would equally well apply to *any* evolutionary track passing through the sdB/sdO domain along the EHB.

In § II, we consider briefly the constraints on pre–white dwarf evolution set by white dwarf observations. We also describe the particular evolutionary sequences used in the present paper. The location of these sequences in a modified H-R diagram is examined in § III. We discuss both the conventional approach of transforming observed quantities into a theoretical H-R diagram and our approach, which consists of transforming stellar evolutionary tracks into the observer's diagram. Illustrative examples of this method, involving the use of available pre–white dwarf evolutionary tracks, are presented. In § IV, we explore some properties of hot subdwarfs evolving along the EHB. We discuss the implications of the observed sdB/sdO transition on the envelope structure of hot subdwarfs, and discuss the problem of element diffusion on the EHB. A preliminary discussion of the constraints imposed by these processes on the evolutionary time scale of hot subdwarfs is also presented. Some speculations concerning the evolutionary phases preceding the hot subdwarf stage are offered in § V, and our conclusions are presented in § VI.

II. THE EVOLUTIONARY MODELS

If, as their location in the H-R diagram suggests, a fraction of or all the hot subdwarfs evolve into white dwarfs, then inferences about the internal composition of white dwarfs can also be extended to the hot subdwarfs. For example, the average mass of the DA white dwarfs is in the range 0.58–0.75 $M_\odot$ (Koester, Schulz, and Weidemann 1979; Shipman and Sass 1980). This not only exceeds the minimum mass for H burning ($\sim 0.085\ M_\odot$; Grossman and Graboske 1971), but also exceeds the minimum core mass for helium ignition at the tip of the red giant branch ($M \sim 0.46$–$0.48\ M_\odot$; Demarque and Mengel 1971*a*; Rood 1972), implying that the white dwarfs are in a post–He-core-burning phase of stellar evolution. However, the average white dwarf mass appears not to exceed the minimum mass for C ignition (1.03 $M_\odot$: Boozer, Joss, and Salpeter 1973), indicating that the core composition of most, if not all, white dwarfs consists of the C/O ashes of the core He-burning stage. The composition of the region immediately above the C/O core should be characteristic of a post–H-burning phase and should consists of nearly pure helium. Overlying all should be a surface layer with primordial composition.

A similar compositional structure can possibly be inferred for the hot subdwarfs, and it thus appears that the masses and composition profile of pre–white dwarf models may be particularly appropriate to the study of hot subdwarf properties. Furthermore, for stars with $M_* \sim 0.6\ M_\odot$, the luminosities reached during the gravitational contraction phases of pre–white dwarf evolution in the absence of nuclear burning appear comparable to those of stars on the EHB (Boozer, Joss, and Salpeter 1973; Winget, Lamb, and Van Horn 1982). Extensive details on these phases are available only for this last set of evolutionary sequences of pre–white dwarf models of 0.4, 0.6, and 0.8 $M_\odot$ with a pure ^{12}C composition. In addition to these homogeneous sequences, details of a 0.6 $M_\odot$ sequence with a carbon core and a compositionally stratified envelope ($10^{-10}\ M_*$ hydrogen layer over a $10^{-5}\ M_*$ helium layer) are also available. These sequences must be regarded in some cases as ad hoc when applied to analyses of the evolutionary status of hot subdwarfs. This is so primarily because no attempt was made by Winget, Lamb, and Van Horn (1982) at being consistent with plausible previous evolutionary phases in the construction of the initial models of these sequences. Thus, for example, the cores of the starting models of each sequence are nondegenerate, while it is known that stars evolving off the horizontal branch have developed degenerate carbon cores (Iben and Rood 1970; Gingold 1974). Thus these models, while suitable for our studies of envelope and atmosphere properties along the EHB, cannot be used for more quantitative studies of the evolutionary state of the hot subdwarfs. Arguments involving specifically evolutionary time scales, for example, must await the availability of relatistic stellar models evolving through that region of the H-R diagram.

The main numerical results from selected models for each sequence are presented in Table 1, and the evolutionary tracks are shown in the theoretical H-R diagram in Figure 1. The basic shapes of all of the evolutionary tracks are qualitatively similar; in particular the 0.6 $M_\odot$ pure ^{12}C and H/He/C sequences do not differ significantly from each other. Also marked on Figure 1 are three models taken from the evolutionary calculations of Boozer, Joss, and Salpeter (1973) for a gravitationally contracting 0.75 $M_\odot$ model with a C/O core. The agreement with these previous calculations is good.

TABLE 1

Properties of Selected Models

$M/M_\odot$ (1)	Model (2)	log R (cm) (3)	log g (cm s^{-2}) (4)	log T_e (K) (5)	log $(L/L_\odot)$ (6)
0.8, C......................	1	10.810	4.41	4.396	2.465
	2	10.439	5.15	4.609	2.573
	3	9.610	6.81	5.054	2.697
	4	8.861	8.30	4.609	−0.579
0.6, C......................	1	10.590	4.72	4.407	2.072
	2	10.371	5.16	4.525	2.103
	3	9.490	6.92	4.960	2.081
	4	8.963	7.97	4.543	−0.641
0.6, H/He/C	1	10.621	4.66	4.392	2.071
	2	10.234	5.43	4.604	2.144
	3	9.623	6.65	4.900	2.108
0.4, C......................	1	10.284	5.16	4.387	1.379
	2	9.804	6.12	4.630	1.387
	3	9.302	7.12	4.708	0.698

Notes.—In column (1), C refers to the pure ^{12}C models, H/He/C to the stratified models. R, T_e, L, g have their usual meaning.

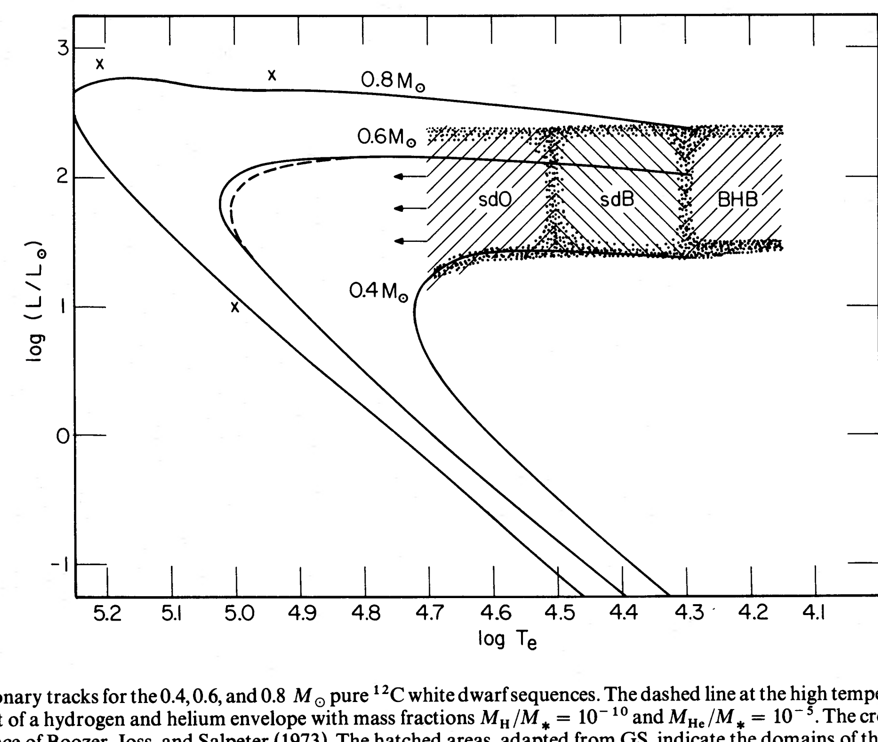

Fig. 1.—Evolutionary tracks for the 0.4, 0.6, and 0.8 $M_\odot$ pure ^{12}C white dwarf sequences. The dashed line at the high temperature end of the 0.6 $M_\odot$ track shows the effect of a hydrogen and helium envelope with mass fractions $M_H/M_* = 10^{-10}$ and $M_{He}/M_* = 10^{-5}$. The crosses are models from the 0.75 $M_\odot$ C/O sequence of Boozer, Joss, and Salpeter (1973). The hatched areas, adapted from GS, indicate the domains of the blue horizontal branch, sdB, and sdO stars from the GS faint blue star survey. The domain boundaries are stippled to emphasize the considerable uncertainties in the exact extent of the individual regions. The arrows indicate the probable extension of the sdO domain to higher effective temperature.

Superposed on the evolutionary tracks of Figure 1 are the areas of the H-R diagram occupied by the blue horizontal branch, sdB, and sdO stars, according to GS. The boundaries are stippled because of the considerable uncertainties in the exact extent of the regions, in particular at large effective temperatures (see GS for a detailed discussion). It is serendipitous that, as pointed out previously, tracks for gravitationally contracting stars with $M_* \sim 0.6\ M_\odot$ traverse the sdB–sdO region of the H-R diagram. To our knowledge, these are the only evolutionary tracks to date which evolve through the hot subdwarf domain along the EHB (see GS; Caloi 1972, 1976; and Sweigart, Mengel, and Demarque 1974 for a summary of previous calculations).

III. THE EVOLUTIONARY TRACKS IN THE H-R DIAGRAM

a) *The Conventional Approach*

GS have discussed extensively the determination of atmospheric parameters and luminosities from their observational material. Photoelectric *UBV* colors are combined to determine the reddening-free parameter, *Q*, whose correlation with the reciprocal effective temperature, θ_e, is calibrated over the range $0.10 < \theta_e < 0.50$. The surface gravity is determined from the measured width $D(x)$ of the Balmer lines at a depression *x*. The variation of $D(0.2)$ with surface gravity has been calibrated with model atmosphere calculations by GS. Once θ_e and log *g* are obtained, the stellar luminosity-to-mass ratio is determined $[L/M \propto (g\theta_e{}^4)^{-1}]$. Absolute bolometric and visual magnitudes are obtained by adopting (i) an average mass for the EHB and (ii) bolometric corrections. GS choose $M_* = 0.66\ M_\odot$ on the EHB.

The transformation from the observed quantities (*UBV* colors, $D[0.2]$) to the theoretical H-R diagram involves some serious uncertainties. The $Q(\theta_e)$ calibration appears unreliable for $T_e > 40{,}000$ K ($\theta_e < 0.13$). Several sdO stars in Table A4 of GS were assigned temperatures that high or higher. Further, the calibration of the $D(x)$ versus *g* relationship is based on an inhomogeneous collection of model atmosphere calculations, involving varying He/H and metal ratios, different line broadening theories, and often different physical assumptions (i.e., blanketed versus unblanketed calculations). In addition, at the time of the analysis of GS, only a few hot, high-gravity models had been computed. Their calibration of $D(0.2)$ versus *g* at $T_e > 30{,}000$ K is thus uncertain.

The influence of these various uncertainties on the determination of $M_{\rm bol}$ is especially important at high effective temperatures. Consequently, several hot O subdwarfs in the GS sample have uncertain gravities and luminosities. In addition, GS point out that the structure of the sdB/sdO transition region is most sensitive to errors in the temperature determination, so that temperature errors could shift stars along the EHB and blur any possible gaps in the distribution of hot EHB stars.

b) *A New Approach*

The uncertainties inherent in the conventional approach have prompted us to investigate an alternative method of analysis. In the present paper, we transform theoretical evolutionary tracks into the appropriate observer's diagram, where a direct comparison with *unprocessed* observations can be performed. In some respects, our approach is similar to that of Newell (1973), who prefers the use of the T_e versus log *g* diagram to the conventional H-R diagram. Nevertheless, his approach still requires some processing of the observational material, since effective temperatures and surface gravities have to be obtained first. We carry this philosophy one step further by working directly in the two-color and in the $(B - V)$ versus $D(0.1)$ of Hγ diagrams. Because the theoretical calculations provide us with exact values of T_e and log *g* at each evolutionary stage, the tracks can be transformed *exactly* into the chosen observer's diagram. In addition, the influence of improvements in the model atmosphere calculations (i.e., inclusion of line blanketing, NLTE effects, or additional opacity sources) can readily be estimated in the observer's diagram.

The recent availability of large homogeneous grids of model atmosphere calculations at the effective temperatures and gravities typical of the hot subdwarfs makes possible a preliminary application of our method to these stars. In the present paper, we have used the detailed grids of blanketed, LTE model atmospheres of Wesemael *et al.* (1980) and Wesemael (1981) for pure hydrogen and pure helium composition, respectively. While only broad conclusions can be drawn from an analysis in terms of monoelemental atmospheres, the bewildering variety of H I, He I, He II, and metal line strengths in hot subdwarf spectra in our estimation precludes such detailed analyses of the EHB at this time. We have therefore chosen to explore the behavior of our evolutionary tracks in terms of the idealized cases of pure hydrogen and pure helium compositions. These results should bracket the behavior of mixed hydrogen-helium atmospheres, which generally appear to characterize the hot subdwarfs as a group.

i) *The Model Atmosphere Calculations*

The hot, high-gravity, pure hydrogen model atmospheres used in the present study all assume LTE and include line blanketing by the Lyman and Balmer series of hydrogen. In practice, only the opacities of the first four members of each series were explicitly sampled with frequency points. For wavelengths shorter than that characterizing the last visible line of a series, the bound-free opacity calculated at the series limit was adopted.

For the color calculations, the emergent fluxes from the model atmosphere calculations were adopted directly. Fluxes at intermediate wavelengths were obtained by spline interpolation, and subsequently folded over the transmission functions of Matthews and Sandage (1963). The color equations of Matthews and Sandage were used.[6] We refer the reader to Wesemael *et al.* (1980) for a

[6] We note that the work of Matthews and Sandage (1963) on the calibration of the broad-band colors has recently been extended by Schulz (1978), who calibrated the broad-band system with the help of the white dwarf standards of Oke (1974). However, because the evolutionary tracks in the pre-white dwarf phases considered here lead to large variations in the surface gravity of the models, and because Schulz's calibration is restricted to white dwarfs, we have chosen to use the Matthews and Sandage calibration throughout.

tabulation of the broad-band colors used and for additional information on the models and color calculations.

Model atmospheres for the helium-rich composition were taken from the grid of hot, high-gravity, pure helium atmospheres of Wesemael (1981). In addition, some models at low gravity ($\log g < 5.0$) were computed specifically for the present work. Again, all models are in LTE, and blanketing by the lines of He I and He II was included in the model computation. Details can be found in Wesemael (1981).

Because the number of lines present in the spectra of helium-rich objects is large, and because of the approximations included in the calculation of the line absorption coefficient in the LTE continuum program, the emergent flux over the restricted range of wavelengths of the *UBV* filters was recomputed in a separate program. This program makes use of the blanketed temperature structure, and uses the best available line broadening theories for both He I and He II lines. For all blanketed models, the emergent flux was recomputed at a set of 252 frequency points in the range $2800 < \lambda(\text{Å}) < 7400$, and 12 He I and seven He II lines were explicitly included in that wavelength range. The emergent fluxes were then folded over the transmission functions of the *UBV* filters. The filter data and color equations used are identical to those used for the pure hydrogen models.

ii) *An Illustrative Example*

As an illustrative example of the new method, we discuss below the behavior of pre–white dwarf evolutionary tracks in the $(U-B)$ versus $(B-V)$ and in the $D(0.1)$ versus $(B-V)$ diagrams. These particular choices are only meant as preliminary illustrations of the potential of our method. Improvements are of course possible as more observational material (e.g., improved spectroscopy, ultraviolet photometry) on the hot subdwarfs and better, or more appropriate, evolutionary tracks become available.

Figure 2*a* shows the path traced by the evolutionary track for the 0.6 $M_\odot$ model in the two-color diagram. An atmospheric composition of pure hydrogen was adopted in this example. Evolution starts from a model in the lower left-hand corner of the diagram, and proceeds upward and to the left. The rise to high effective temperatures for these models is nearly vertical. This is because $U-B$ is very sensitive to T_e in that range of effective temperatures. The variation of $B-V$, however, is regulated by the fact that $B-V$ reddens with increasing gravity but gets bluer with increasing effective temperature in that range (Wesemael *et al.* 1980). These two effects work in opposite directions and combine to yield a small $B-V$ variation along the track. The detailed structure of this branch could be affected by the presence of metals, which are omitted in the present calculations. One could perhaps expect the increased ultraviolet opacity in the metal-rich models to redden $U-B$ somewhat at a fixed $B-V$. The colors on the ascending branch will be only slightly affected by NLTE effects. At the temperatures and gravities of interest ($\log T_e > 4.6$ at $\log g > 5.5$), the NLTE calculations of Kudritzki (1976), Wesemael *et al.* (1980), and Wesemael (1981) for a variety of chemical compositions give NLTE vectors of $\Delta(U-B) < 0.02$ mag and $\Delta(B-V) < 0.01$ mag.

After reaching the point of maximum effective temperature, the track turns over, and cooling proceeds at nearly constant radius. On that cooling branch, both $U-B$ and $B-V$ are temperature sensitive and the gravity is fixed. Qualitatively similar tracks are found when the pure-helium model atmospheres are employed.

The path traced by the 0.6 $M_\odot$ sequence in the EHB domain is shown on Figure 2*b* for both the pure hydrogen and the pure helium atmospheres. Superposed on these tracks are the observations of Greenstein (1976) of hot B and O subdwarfs. It seems suggestive that most of the hot subdwarfs, with atmospheric compositions intermediate between our pure hydrogen and pure helium extremes, lie between, or close to, the two evolutionary paths plotted. Further, the sdB's preferentially populate the redder part of the area between the two lines. Several objects lie to the right of the expected EHB domain and could be reddened.

Because the *UBV* colors in the temperature range considered are not very sensitive to surface gravity, the two-color diagram will not be a useful mass-discriminant for models evolving along the EHB. Line widths, however, are sensitive to $\log g$. Figure 3 shows the behavior of the evolutionary tracks at $M_*/M_\odot = 0.4, 0.6$, and 0.8 in the $D(0.1)$ of Hγ versus $(B-V)$ diagram. An atmospheric composition of pure hydrogen is assumed. Also shown are the sdB observations of Greenstein (1976). The measured line widths suggest an average surface gravity for the sdB stars of the order of $\log g \approx 5$, in agreement with the result of GS (see their Fig. 12*a*). As in the two-color diagram, the observational material has not been corrected for possible reddening.

IV. THE PROPERTIES OF EVOLVING HOT SUBDWARFS

Although the existence of a layered structure can reasonably be assumed for the hot subdwarfs, the specific masses of the outer layers will depend on the extent of the core burning phases, on the subsequent shell burning phases, and upon the details of possible prior mass loss. However (as discussed in a preliminary analysis by Winget and Cabot 1980), if we wish to identify the hot subdwarfs as an evolutionary sequence, the transition between the sdB and sdO photospheric chemical compositions, which we postulate is due to convective mixing, provides stringent constraints on the thickness of the outer, hydrogen-rich surface layer in these stars.

a) *The sdB/sdO Transition: A Convective Mixing Phase?*

Winget and Cabot (1980) have investigated the problem of convective mixing across the composition boundary between an outer layer of solar composition and an underlying helium layer for the 0.6 $M_\odot$ pre–white dwarf evolutionary sequence. The actual compositions assumed were the Iben 17 ≡ I17 mixture ($X = 0.80$, $Y = 0.18$, Cox and Stewart 1970*a*) in the outermost region and an almost pure helium mixture (Iben V, $X = 0.000$,

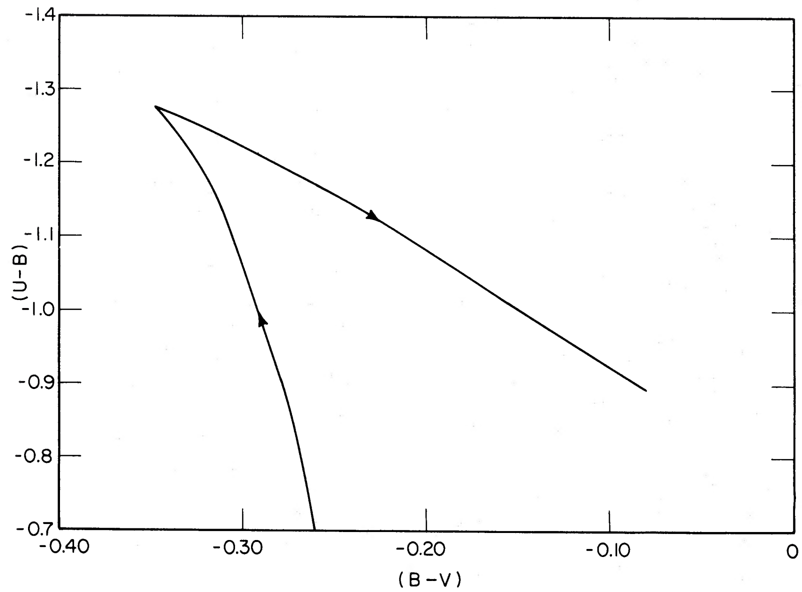

FIG. 2*a*

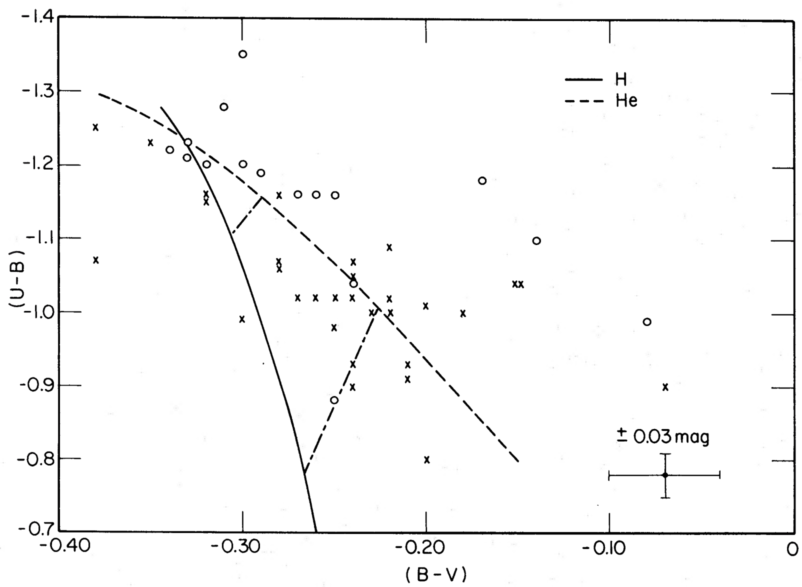

FIG. 2*b*

FIG. 2.—(*a*) Path traced by the evolutionary track of the 0.6 $M_\odot$ model in the broad-band two-color diagram. An atmospheric composition of pure hydrogen is assumed. Both the EHB contraction phase (*lower left branch*) and the white dwarf cooling phase (*upper right branch*) are shown. The arrows denote the direction of evolution. (*b*) The broad-band two-color diagram of the hot O and B subdwarfs. The crosses denote sdB stars; the open circles, the sdO stars. Also shown are the theoretical EHB branches for the 0.6 $M_\odot$ model, obtained with pure hydrogen (*solid line*) and pure helium (*dashed line*) atmospheres. The dash-dotted lines are the boundaries of the region between log $T_e = 4.3$ and log $T_e = 4.5$. The observational data points are from Greenstein (1976). The error bars correspond to an error of ± 0.03 mag in both colors.

$Y = 0.999$, Cox and Stewart 1970*b*) in the region underneath. In summary, Winget and Cabot found the following:

1. A transition from a hydrogen-rich to a helium-rich surface composition is possible only if the I17 layer is less massive than approximately 10^{-8} M_* for models with log $T_e > 4.1$ (appropriate to the EHB region). For more massive I17 layers, convection does not extend down to the composition boundary and mixing cannot occur in this temperature range.

2. A helium mass fraction $Y \gtrsim 0.1$ at the bottom of the overlaying 117 layer is required for convection to cross over the composition boundary. Partial ionization of hydrogen is not by itself sufficient to generate an extensive enough convection zone in the outermost layer of hot subdwarf models.

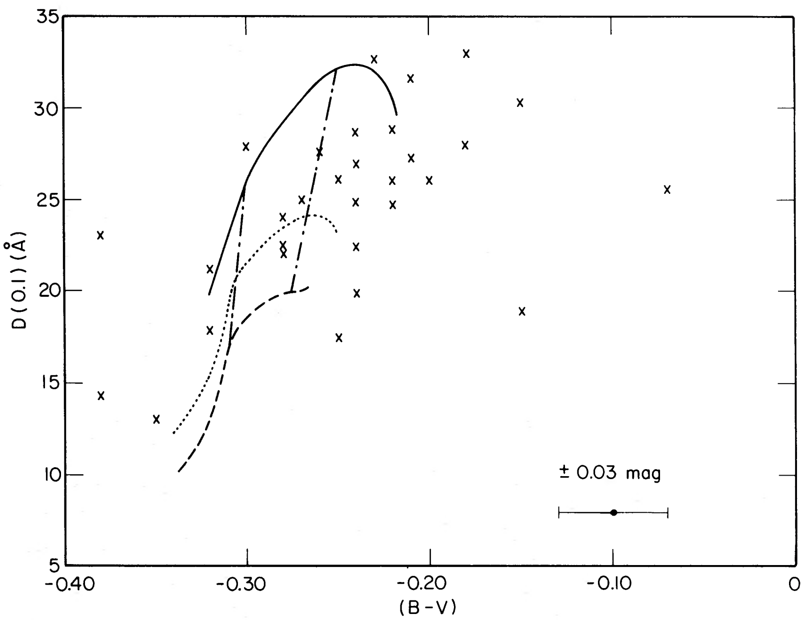

FIG. 3.—Variation of the full width of Hγ at a depression of 0.1 as a function of $(B-V)$ for the theoretical evolutionary sequences used in this paper. The blanketed model atmospheres calculations for a pure hydrogen composition are used. The solid curve is for the 0.4 $M_\odot$ model, the dotted curve for the 0.6 $M_\odot$ model, and the dashed curve for the 0.8 $M_\odot$ model. The dash-dotted lines are the boundaries of the region $4.3 \leq \log T_e \leq 4.5$, characteristic of the hot B subdwarfs (GS). The crosses are the observational values for the B subdwarfs of GS, taken from Greenstein (1976). The error bar corresponds to an uncertainty of ± 0.03 mag in $(B-V)$.

3. When mixing occurs across the composition boundary, it is the result of the confluence of a He II–He III convection zone present in the I17 layer with an underlying He II–He III convection zone in the helium layer.

4. The effective temperature at which mixing first occurs depends on the mass of the I17 layer. Thus mixing is possible at $\log T_e > 4.1$ for $M_{117} < 10^{-8}\, M_*$. However, the postmixing He II–He III convection zone, bringing with it helium-rich material, does not reach the observable stellar surface ($\tau \approx 1$) until $\log T_e \approx 4.5$.

To investigate the sensitivity of these results to variations in basic stellar parameters, we have extended the calculations of Winget and Cabot (1980) to the 0.4 and 0.8 $M_\odot$ models. Static envelope models with a representative value of $M_{117}/M_* = 10^{-10}$ were computed for the gravities and effective temperatures appropriate to the evolutionary sequences. Figures 4 and 5, which show the structure of the convection zones in these envelope models as a function of effective temperature, summarize the results of these calculations. Mixing occurs at $\log T_e \gtrsim 4.28$ for the 0.8 $M_\odot$ models, and at $\log T_e \gtrsim 4.19$ for the 0.4 $M_\odot$ models. However, in both cases the top of the convection zone is located well below the photosphere (the dash-dotted line indicates approximately the depth where $\tau = 1$) and the helium-rich material in the mixed regions is then not visible in the atmosphere. Note that the present envelope models are static and that, consequently, the evolution of the He II–He III convection zone after mixing is not exactly that shown in the figures. From the work of Winget and Cabot (1980), however, we expect the following general trend: After mixing, the convection zone gets thinner and closer to the surface as a result of an overall increased helium ionization in the envelope due to the star's evolution. Eventually, convection breaks through the photosphere, and the atmosphere then assumes a helium-rich composition. The present results coupled with those of Winget and Cabot (1980) indicate that helium-rich material becomes visible in the range $\log T_e \approx 4.5$–4.6 for models with parameters appropriate to masses ranging from 0.4 to 0.8 $M_\odot$. This is in excellent agreement with the observed sdB/sdO transition in surface chemical composition of hot subdwarfs.

Our calculations also indicate that for stars with surface gravities larger than those appropriate to the 0.4 $M_\odot$ model, convection may shut off before breaking through the photosphere. Indeed, Figure 5 shows that convection shuts off before any appreciable convective penetration above $\tau \approx 1$ can occur. *This suggests that for models with* $\log g \gtrsim 5.6$, *a sdB/sdO transition due to a mixing episode is not possible.* If the sdB/sdO transition is indeed due to convective mixing, the majority of hot B subdwarfs should have surface gravities lower than this limit. We have also verified that convective overshooting is ineffective in bringing helium-rich material to the surface before the convection zone breaks $\tau \approx 1$, at $\log T_e \approx 4.5$–4.6. This confirms and extends the results of Winget and Cabot (1980).

b) Diffusion and Surface Helium Abundances

Along with convection, diffusion is another mechanism that may alter the surface chemical composition of hot subdwarfs. In particular, in the range $4.1 \lesssim \log T_e \lesssim 4.5$, the downward diffusion of helium through the upper hydrogen-rich layer may be quite important.

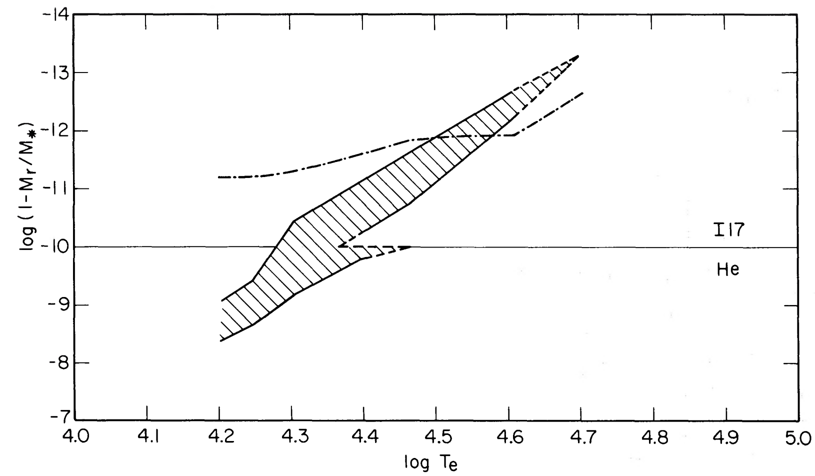

FIG. 4.—The convection zone structure in the envelope of the 0.8 $M_\odot$ model. The fractional mass is shown as a function of effective temperature. An Iben 17 composition and a mass fraction $M_{\rm I17}/M_* = 10^{-10}$ were assumed for the upper hydrogen-rich layer. The hatched area indicates the presence of convection. The location of $\tau \approx 1$ (*dash-dotted line*) is approximate. The dashed convection zone boundaries indicate an approximate extrapolation required by the disappearance of the convection zone between two models from the grid.

Helium may diffuse through hydrogen via gravitational settling, thermal diffusion, and radiative forces. We first estimate the upward radiative acceleration on helium with the help of fitting formulae developed by Michaud *et al.* (1979). We use their equations (7) and (17), which provide an estimate that is accurate within a factor of 1.5 for a range of density-temperature given by their equation (18), and for helium number abundances ranging from 10^{-4} to 0.1 in ionized hydrogen. These conditions are always largely verified in the atmospheres and envelopes of hot subdwarfs models: the densities and temperatures encountered are always within the range of the fitting formulae, the helium number abundance in the I17 mixture is ~ 0.05, hydrogen is essentially completely ionized, and helium is mostly singly ionized. Radiative accelerations on helium have been evaluated in a representative model for each of the three evolutionary sequences. (The actual models considered are the ones just prior to mixing.) In all cases the radiative acceleration at the photosphere is less than $\sim 2\%$ of the surface gravity. Since radiative forces on helium actually decrease with depth in our models, they can be safely neglected here.

Diffusion time scales due to gravitational settling and thermal diffusion are computed following Fontaine and Michaud (1979). In these calculations, diffusion is assumed to operate without competition from other mechanisms, and singly ionized helium is treated as a trace element in a hydrogen ion background. Under the conditions encountered in hot subdwarf envelope models, thermal diffusion is found to be small compared to gravitational settling.

The time scale for helium to diffuse downward below $\tau = 1$ in the I17 mixture was found previously by Winget and Cabot (1980) to be $\sim 2 \times 10^4$ years for a representative model at log $T_e \approx 4.3$ in the 0.6 $M_\odot$ sequence. For

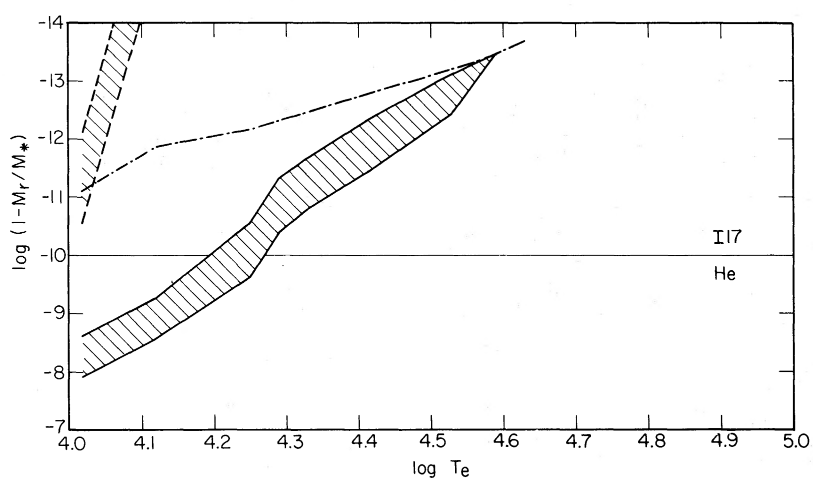

FIG. 5.—Same as Fig. 4, but at $M = 0.4\ M_\odot$. Note that, near log $T_e \approx 4.55$, convection seems to shut off close to the effective temperature where the top of the convection zone first reaches $\tau \approx 1$. This could imply that, in this model, the convectively mixed helium-rich material will not reach the photosphere before convective mixing turns off.

diffusion of helium down to depths $\Delta M = 10^{-10}\ M_*$, however, the characteristic time scale is $\sim 1 \times 10^5$ years. These computations have now been extended to the 0.4 and 0.8 $M_\odot$ sequences. For the 0.8 $M_\odot$ model, the characteristic diffusion time scales are $\sim 6 \times 10^4$ years for diffusion down to $\tau \sim 1$, and $\sim 3 \times 10^5$ years for diffusion down to $\Delta M = 10^{-10}\ M_*$. For the 0.4 $M_\odot$ models, however, the helium diffusion time scale through $\tau \approx 1$ is quite short, only $\sim 4 \times 10^3$ years. Even through a depth $\Delta M = 10^{-10}\ M_*$, the diffusion time scale is only $\sim 5 \times 10^4$ years.

Our analysis thus suggests that typical helium diffusion time scales through the photosphere of stars evolving along the EHB will be of order of a few times 10^3 to a few times 10^4 years. It is not possible, at this stage, to follow the time-dependent evolution of the envelope composition since (i) the evolutionary time scales through the hot subdwarf phases are uncertain (see § IV*d*) and (ii) time-dependent mixing calculations are not available. A full exploration of the temperature dependence and stellar mass dependence of the helium deficiency through the sdB phase must await the result of these calculations.

c) Hot Subdwarfs as Progenitors of Helium-rich White Dwarfs?

As the evolution proceeds toward higher effective temperatures, convection eventually shuts off. This is found to occur in the range log $T_e \approx 4.7$–4.8 for the 0.8 and 0.6 $M_\odot$ models (Fig. 4 and Winget and Cabot 1980). After convection has ceased, one might *a priori* expect that hydrogen and helium will tend to segregate again. Since hydrogen is very highly diluted in the He II–He III convection zone after mixing has occurred, it is then appropriate to estimate upward diffusion time scales of ionized hydrogen treated as a trace ion in a background of completely ionized helium. Computations for a representative envelope model at $M_* = 0.6\ M_\odot$ near log $T_e \approx 4.7$ indicate that the hydrogen diffusion time scale is short, of the order of 6×10^4 years for upward diffusion through $\Delta M = 10^{-9}\ M_*$, and $\sim 2 \times 10^4$ years for diffusion through $\Delta M = 10^{-10}\ M_*$. Thus hydrogen might be expected to reappear quickly in the atmospheres of these stars after convection has stopped.

However, a mechanism exists that may be capable of expelling the hydrogen completely from a subdwarf O star. After mixing has occurred, hydrogen is a trace ion in a background of ionized helium. The local electric field in the atmosphere is specified by the main constituent (helium); and a proton, for example, will feel an electric force larger than its weight and directed *outward*. In singly ionized helium, the electric force on a proton would be twice as large as the gravitational force. Hydrogen ions are consequently torn away from the star (Michaud and Fontaine 1979). However, in order to maintain the process, electric neutrality must be preserved in the outgoing stellar wind. This is possible if the star is surrounded by a sufficiently hot corona that allows as many electrons as protons to escape from the star. Michaud and Fontaine (1979) have found that a proton flux as high as $\sim 10^{15}$ cm^{-2} s^{-1} can be maintained in helium-rich stars provided the coronal temperature is $T \gtrsim 10^6$ K (see, however, an opposing viewpoint by Alcock 1980). This corresponds to a hydrogen mass loss rate of about $10^{-12}\ M_\odot$ yr^{-1} for a representative model of the 0.6 $M_\odot$ sequence. This estimate leads to a short time scale for hydrogen to be completely expelled in the sdO phase ($\tau \lesssim 10^4$ years). While the energy source of the postulated corona remains unknown, it is tempting to speculate that acoustic noise generation in the He II–He III convection zone in the early sdO phase could be responsible for the coronal heating.

If this scenario is accurate, hot subdwarfs may provide a mechanism for producing helium-rich white dwarfs. An observational search for coronae around hot subdwarfs would be a test of this hypothesis.

d) Constraints on the Evolutionary Time Scales of B Subdwarfs

The assumptions that (i) the EHB represents an evolutionary sequence, and (ii) hot sdO stars evolve into white dwarfs allow us to use the results of the preceding sections to place some limits on the evolutionary time scales on the EHB.

A lower limit on the evolutionary time scale of sdB stars can be obtained by assuming that all sdB stars evolve into white dwarfs. We use the observed space density of B subdwarfs ($n_{\rm sdB} = 1.4 \times 10^{-9}$ pc^{-3}; Green 1977) and the white dwarf birthrate of Weidemann (1977), $\chi_{\rm WD} = 2 \times 10^{-12}$ pc^{-3} yr^{-1}, to obtain $\tau_{\rm sdB} > 7 \times 10^2$ yr. On the other hand, the fact that sdB stars are helium-poor, but still contain detectable amounts of helium, implies that the evolutionary time scale through the sdB phase cannot be much longer than the helium diffusion time scale through $\tau \sim 1$ in that phase. According to the calculations of § IV*b*, we estimate the evolutionary time scale of the B subdwarfs to be $\tau_{\rm sdB} \lesssim 10^5$ years. Thus, within the framework of assumptions (i) and (ii), the lifetime of the sdB phase appears quite effectively constrained. We also note that the observed ratio of space densities of B subdwarfs to O subdwarfs (Green 1977) places a further constraint on the evolutionary time scales in these phases ($\tau_{\rm sdO}/\tau_{\rm sdB} \sim 2.4$). This constraint will have to be satisfied by any sequence evolving along the EHB which endeavours to explain the hot subdwarfs.

V. SOME SPECULATIONS ON PRE-HOT-SUBDWARF EVOLUTION

From a reanalysis of the kinematical data available on 17 B subdwarfs, Baschek and Norris (1975) concluded that these stars are a mixture of a halo and of an old disk population. The same conclusion was reached in GS's analysis of the subdwarf O stars. A similar kind of population admixture is also observed in white dwarfs (Liebert 1980), although the latter appear to belong mostly to an old disk population. An important constraint on our evolutionary scheme is thus the fact that, as pointed out by Baschek and Norris (1975), the progenitors of a large fraction of the hot subdwarfs could be disk objects with mass $M \sim 1.0$–$1.5\ M_\odot$ at the main sequence turnoff.

With a core composed of elements heavier than helium, the hot subdwarfs must be in a post–horizontal branch evolutionary phase. They may, however, have bypassed the asymptotic giant branch evolutionary phase, since double-shell source objects with core masses of 0.6–0.8 $M_\odot$ reach luminosities (log $[L/L_\odot] \sim 4$; Paczyński 1971) that are much too high to be identified with the hot subdwarf stars (GS). The mass loss required ($> 0.2\ M_\odot$) to explain the EHB stars must then be achieved by steady mass loss only (i.e., no planetary nebula–like envelope ejection). This is not implausible, since standard stellar evolution already requires that $\sim 0.2\ M_\odot$ be lost between the main sequence and the horizontal-branch phases to explain the morphology of the horizontal branch in globular clusters (Iben and Rood 1970; Demarque and Mengel 1971*b*); this mass loss is steady and occurs presumably during the ascent of the first giant branch.

Interestingly, the bypassing of the asymptotic giant branch proposed to avoid a horizontal crossing of the H-R diagram at too high a luminosity can perhaps be qualitatively understood within the framework of standard stellar evolution. Detailed calculations of the post–zero-age horizontal-branch evolution of low-mass, metal-poor ($Z \leq 0.001$) stars have been carried out by Iben and Rood (1970), Strom *et al.* (1970), Sweigart, Mengel, and Demarque (1974), Gingold (1974), Sweigart and Gross (1976), and others. A model at $M = 0.625\ M_\odot$, $Y = 0.30$, and $Z = 0.001$ of Iben and Rood (1970), for which detailed information is available, shows the following behavior: after an initial redward excursion, evolution off the zero-age horizontal branch proceeds blueward, until log $T_e \approx 3.95$, log $(L/L_\odot) \approx 1.65$. Following helium core exhaustion, the track then turns over, and the star evolves to the red in the H-R diagram and brightens. After another blueward excursion, the star reaches the base of the AGB (log $T_e \approx 3.75$, log $[L/L_\odot] \approx 1.9$). At this point, the mass interior to the center of the helium-burning shell is only about 0.15 $M_\odot$. As the star evolves up the AGB, the carbon-oxygen core grows. The model was followed until log $(L/L_\odot) \approx 2.35$, at which point the mass of the C/O core is $\sim 0.38\ M_\odot$ (qualitatively similar tracks are seen at higher mass, i.e., 0.85 $M_\odot$). The evolution near the base of the AGB proceeds rather slowly, as shown by Strom *et al.* (1970) who first identified some of the supra–horizontal branch stars observed in globular clusters with this evolutionary phase (also Sweigart, Mengel, and Demarque 1974). Stars in this area of the diagram burn helium in one shell and hydrogen in another.

If the helium and hydrogen envelope masses are small, double shell burning could consume all the available nuclear fuel before the star evolves too far up the AGB. In that case, both shells will extinguish and the star could evolve horizontally to the blue, passing through the hot subdwarfs at log $(L/L_\odot) \sim 2$. This speculative evolution has some similarities with that of the 0.51 $M_\odot$ post–zero-age horizontal branch model of Sweigart, Mengel, and Demarque (1974). It is perhaps suggestive that the hydrogen layer mass required for convective mixing to occur near the sdB/sdO boundary ($M/M_* \lesssim 10^{-8}$) is indeed too small to support any significant hydrogen-shell burning.

VI. SUMMARY AND CONCLUDING REMARKS

We have carried out a reinvestigation of the properties and evolutionary status of the hot O and B subdwarfs in terms of recent homogeneous grids of hot, high-gravity atmospheres and of detailed convective envelope calculations appropriate to stars evolving through the hot subdwarf region along the EHB. We have outlined an alternative method of analysis of the hot subdwarfs, where the comparison between theoretical evolutionary tracks and observations is carried out as close to the fundamental observational results as possible. For the purpose of illustration, we discussed a set of pre–white dwarf sequences at $M_*/M_\odot = 0.4$, 0.6, and 0.8 which evolve along the EHB through the observed hot subdwarf domain. We reach the following conclusions:

1. Our analysis supports the contention of GS that hot subdwarfs have masses characteristic of low-mass, evolved stars ($M_* \sim 0.6\ M_\odot$). Improved mass estimates could be obtained when realistic evolutionary tracks and additional observational material become available. There is, in particular, a need for more homogeneous photometric observations.

2. Along evolutionary tracks through the hot subdwarf domain, convective mixing provides a natural explanation of the observed sdB/sdO composition transition, provided that the mass of the upper hydrogen-rich layer does not exceed $\sim 10^{-8}\ M_*$ (see also Winget and Cabot 1980). Is this scheme, the observed sdB/sdO transition, which occurs near log $T_e \approx 4.5$, coincides with the appearance near $\tau \approx 1$ of helium-rich material mixed from the underlying helium envelope. We have also carried out preliminary estimates of the importance of element diffusion in the envelopes of hot subdwarfs. At the photospheres of sdB's helium will diffuse downward on short time scales ($\sim 10^4$ years). This may lead to helium deficiencies in the atmospheres of hot B subdwarfs that get larger as the effective temperature increases. While precise predictions still await the results of detailed time-dependent mixing calculations and improved evolutionary calculations, this expected trend is potentially observable. Spectrophotometric data should be obtained for a selected number of sdB stars and analyzed with model atmosphere techniques.

3. We have speculated on the fate of the diluted hydrogen in the sdO phase. Hydrogen could be expelled from a hot O subdwarf according to the mechanism proposed by Michaud and Fontaine (1979) if the star is surrounded by a hot corona. This suggests an observational search for possible coronae around sdO stars. If hydrogen is indeed efficiently expelled in these objects, hot subdwarfs could then be progenitors of helium-rich white dwarfs.

4. An upper limit of $\tau_{\rm sdB} \sim 10^5$ yr on the lifetime of the sdB phase can be set on the basis of diffusion arguments.

This limit, along with Green's (1977) observed value of the space density of sdB stars, implies a sdB birthrate $\chi_{sdB} \gtrsim 1.4 \times 10^{-14}$ pc^{-3} yr^{-1}. This, in turn, suggests that at least 1% of all white dwarfs pass through the hot subdwarf phase. This particular result could be made more definite with the availability of detailed evolutionary calculations using initial models consistent with expected previous evolutionary phases. Thus we cannot, at this stage, exclude the possibility that *all* helium-rich white dwarfs descend from hot subdwarfs (see, however, the alternative mechanism suggested by Nather, Robinson, and Stover 1981).

5. Likely candidates for the progenitors of the hot subdwarfs could be post-ZAHB stars with low helium and hydrogen envelope masses. The low envelope masses suggests that these stars will not climb too far up the AGB, where double shell burning is the main energy source. Detailed post–zero-age horizontal-branch evolutionary calculations for models with low envelope masses will be necessary to ascertain whether this pre–hot subdwarf evolution scheme is reasonable.

We thank J. L. Greenstein for providing us with a copy of his faint blue star catalog, and G. Michaud for discussions. We acknowledge the initial contribution of M. P. Savedoff whose ideas and interest over the years laid the foundations for this work. This work was supported in part by NSF grants AST 79-09391 (Rochester), AST 78-20123 and AST 80-18198 (Illinois), by the Conseil de Recherches en Sciences Naturelles et Génie Canada, and by the Ministère de l'Education du Québec. F. W. thanks M. J. Rees for his hospitality at the Institute of Astronomy, where part of this work was carried out. W. C. is grateful to W. M. Sparks for his hospitality at the Goddard Space Flight Center.

REFERENCES

Alcock, C. 1980, *Ap. J.*, **242**, 710.
Baschek, B., and Norris, J. 1975, *Ap. J.*, **199**, 694.
Boozer, A. H., Joss, P. C., and Salpeter, E. E. 1973, *Ap. J.*, **181**, 393.
Caloi, V. 1972, *Astr. Ap.*, **20**, 357.
———. 1976, *Astr. Ap.*, **50**, 471.
Cox, A. N., and Stewart, J. N. 1970*a*, *Ap. J. Suppl.*, **19**, 243.
———. 1970*b*, *Ap. J. Suppl.*, **19**, 261.
Cox, J. P., and Salpeter, E. E. 1961, *Ap. J.*, **133**, 764.
Demarque, P., and Mengel, J. G. 1971*a*, *Ap. J.*, **164**, 317.
———. 1971*b*, *Ap. J.*, **164**, 469.
Faulkner, J. 1972, *Ap. J.*, **173**, 401.
Fontaine, G., and Michaud, G. 1979, *Ap. J.*, **231**, 826.
Gingold, R. A. 1974, *Ap. J.*, **193**, 177.
Green, R. F. 1977, Ph.D. thesis, California Institute of Technology.
Greenstein, J. L. 1976, private communication.
Greenstein, J. L., and Sargent, A. I. 1974, *Ap. J. Suppl.*, **28**, 157 (GS).
Grossman, A. S., and Graboske, H. C. Jr. 1971, *Ap. J.*, **164**, 475.
Hunger, K., Gruschinske, J., Kudritzki, R. P., and Simon, K. P. 1981, *Astr. Ap.*, **95**, 244.
Iben, I., Jr., and Rood, R. T. 1970, *Ap. J.*, **161**, 587.
Koester, D., Schulz, H., and Weidemann, V. 1979, *Astr. Ap.*, **76**, 262.
Kudritzki, R. P. 1976, *Astr. Ap.*, **52**, 11.
Kudritzki, R. P., and Simon, K. P. 1978, *Astr. Ap.*, **70**, 653.
Lamb, D. Q., and Van Horn, H. M. 1975, *Ap. J.*, **200**, 306.
Liebert, J. 1980, *Ann. Rev. Astr. Ap.*, **18**, 363.
Matthews, T. A., and Sandage, A. R. 1963, *Ap. J.*, **138**, 30.
Mengel, J. G., Norris, J., and Gross, P. G. 1975, *Ap. J.*, **204**, 488.
Michaud, G., and Fontaine, G. 1979, *Ap. J.*, **229**, 694.
Michaud, G., Montmerle, T., Cox, A. N., Magee, N. H., Hodson, S. W., and Martel, A. 1979, *Ap. J.*, **234**, 206.
Nather, R. E., Robinson, E. L., and Stover, R. J. 1981, *Ap. J.*, **244**, 269.
Newell, B. 1973, *Ap. J. Suppl.*, **26**, 37.
Oke, J. B. 1974, *Ap. J. Suppl.*, **27**, 21.
Paczyński, B. 1971, *Acta Astr.*, **21**, 417.
Rood, R. T. 1972, *Ap. J.*, **177**, 681.
Schulz, H. 1978, *Astr. Ap.*, **68**, 75.
Shipman, H. L., and Sass, C. A. 1980, *Ap. J.*, **235**, 177.
Strom, S. E., Strom, K. M., Rood, R. T., and Iben, I., Jr. 1970, *Astr. Ap.*, **8**, 243.
Sweigart, A. V., and Gross, P. G. 1976, *Ap. J. Suppl.*, **32**, 367.
Sweigart, A. V., Mengel, J. G., and Demarque, P. 1974, P. 1974, *Astr. Ap.*, **30**, 13.
Weidemann, V. 1977, *Astr. Ap.*, **61**, L27.
Wesemael, F. 1981, *Ap. J. Suppl.*, **45**, 177.
Wesemael, F., Auer, L. H., Van Horn, H. M., and Savedoff, M. P. 1980, *Ap. J. Suppl.*, **43**, 159.
Winget, D. E., and Cabot, W. 1980, *Ap. J.*, **242**, 1166.
Winget, D. E., Lamb, D. Q., and Van Horn, H. M. 1982, in preparation.

W. Cabot and H. M. Van Horn: Department of Physics and Astronomy, University of Rochester, Rochester, NY 14627

G. Fontaine and F. Wesemael: Départment de Physique, Université de Montréal, C.P. 6128, Succ. A, Montréal, Québec, Canada H3C 3J7

D. E. Winget: Department of Astronomy, University of Texas, Austin, TX 78712